Antiviral Research 91 (2011) 167–176

Contents lists available at ScienceDirect

Antiviral Research

journal homepage: www.elsevier.com/locate/antiviral

Resistance to raltegravir highlights integrase mutations at codon 148 in conferring cross-resistance to a second-generation HIV-1 integrase inhibitor

Olivia Goethals [a], Marcia Van Ginderen [a], Ann Vos [a], Maxwell D. Cummings [a], Koen Van Der Borght [a], Liesbeth Van Wesenbeeck [a], Maxim Feyaerts [a], Ann Verheyen [a], Veerle Smits [a], Marnix Van Loock [a], Kurt Hertogs [a], Dominique Schols [b], Reginald F. Clayton [a,*]

[a] Tibotec Virco Virology BVBA, Turnhoutseweg 30, 2340 Beerse, Belgium
[b] Rega Institute for Medical Research, Katholieke Universiteit Leuven, Minderbroederstraat 10, 3000 Leuven, Belgium

ARTICLE INFO

Article history:
Received 9 March 2011
Revised 25 May 2011
Accepted 26 May 2011
Available online 12 June 2011

Keywords:
HIV-1
Integrase
Raltegravir
Resistance
MK-2048

ABSTRACT

Raltegravir is the first integrase strand-transfer inhibitor (INSTI) approved for use in highly active antiretroviral therapy (HAART) for the management of HIV infection. Resistance to antiretrovirals can compromise the efficacy of HAART regimens. Therefore it is important to understand the emergence of resistance to RAL and cross-resistance to other INSTIs including potential second-generation INSTIs such as MK-2048.

We have now studied the question of whether *in vitro* resistance selection (IVRS) with RAL initiated with viruses derived from clinical isolates would result in selection of resistance mutations consistent with those arising during treatment regimens with HAART containing RAL. Some correlation was observed between the primary mutations selected *in vitro* and during therapy, initiated with viruses with identical IN sequences. Additionally, phenotypic cross-resistance conferred by specific mutations to RAL and MK-2048 was quantified. N155H, a RAL-associated primary resistance mutation, was selected after IVRS with MK-2048, suggesting similar mechanisms of resistance to RAL and MK-2048. This was confirmed by phenotypic analysis of 766 clonal viruses harboring IN sequences isolated at the point of virological failure from 106 patients on HAART (including RAL), where mutation Q148H/K/R together with additional secondary mutations conferred reduced susceptibility to both RAL and MK-2048. A homology model of full length HIV-1 integrase complexed with viral DNA and RAL or MK-2048, based on an X-ray structure of the prototype foamy virus integrase–DNA complex, was used to explain resistance to RAL and cross-resistance to MK-2048. These findings will be important for the further discovery and profiling of next-generation INSTIs.

1. Introduction

During the past three decades, the combination of antiretroviral drugs in HAART regimens has transformed the management of human immunodeficiency virus (HIV) infection from a fatal disease to a manageable chronic condition (Palella et al., 1998; Richman, 2001). HAART regimens are designed to suppress viral replication. However resistance to antiretrovirals may develop, resulting in incomplete suppression of HIV (DeGruttola et al., 2000; Richman, 2006). The emergence of resistance to antiretrovirals depends on genetic variation of the virus and the selection of drug-resistant strains during antiretroviral therapy (Paredes and Clotet, 2010). The error-prone nature of the viral reverse transcriptase (3.4×10^{-5} mutations per bp per cycle), which lacks an exonucleolytic proofreading function enables adaptation to drug pressure and the emergence of resistant virus. However, mutations conferring reduced susceptibility to the drug may also compromise the replication capacity or fitness of the virus, and mutations may arise that reduce the degree of susceptibility of the virus to the drug (primary mutations) or compensate for the reduced fitness induced by the initial mutations (compensatory mutations) (Clavel and Hance, 2004; Paredes and Clotet, 2010).

HIV-1 integrase (IN) is an attractive target for antiretroviral drug discovery (Chen et al., 2002; Esposito and Craigie, 1999), by virtue of essentiality to the HIV lifecycle (LaFemina et al., 1992; Sakai et al., 1993) and, moreover, having no close cellular homologues apart from the V(D)J polynucleotide recombinase RAG1/2 (van Gent et al., 1996). Beta-diketo acids were the first investigational IN inhibitors reported, which preferentially block the strand-transfer step of the integration reaction (Hazuda et al., 2000). Recent progress has resulted in the discovery and development of

* Corresponding author. Tel.: +32 14 641443; fax: +32 14 605522.
E-mail address: rclayton@its.jnj.com (R.F. Clayton).

0166-3542/$ - see front matter © 2011 Elsevier B.V. All rights reserved.
doi:10.1016/j.antiviral.2011.05.011

elvitegravir (EVG) (Sato et al., 2006), currently undergoing phase III clinical development in treatment-experienced patients (No authors listed, 2008), and raltegravir (RAL), the first IN inhibitor approved for use in treatment-experienced in the US and Europe and treatment-naive patients in the US (No authors listed, 2009; Cocohoba, 2009; Eron et al., 2010; Lennox et al., 2010, 2009). The IN inhibitor S/GSK1349572 was discovered more recently, and is currently in phase III clinical development in treatment-naïve and treatment-experienced patients (Vandeckerckhove, 2010). Currently approved and investigational IN inhibitors are considered to be IN strand-transfer inhibitors (INSTIs), coordinating to the two Mg^{2+} cations in the IN catalytic site, thereby stabilizing the macromolecular IN–DNA complex at the 3′-processing step of the reaction, leading to prevention of the IN strand-transfer catalytic step (Neamati et al., 2002; Pommier et al., 2005).

HIV-1 resistance to RAL *in vivo* is associated with three distinct genetic pathways defined by the signature IN mutations Y143C/H/R, Q148H/K/R or N155H (Cooper et al., 2008; Johnson et al., 2009). *In vivo* resistance to EVG is associated with the HIV-1 IN mutations T066I, E092Q, Q148K/R and N155H (McColl et al., 2007). *In vitro* and *in vivo* studies revealed common mutations arising with RAL and EVG (Goethals et al., 2008, 2010; Paredes and Clotet, 2010). Similarities in the pharmacophores and resistance profiles of RAL and EVG highlight the need for second-generation INSTIs; inhibitors with superior resistance profiles and higher genetic barriers to the development of resistance. Research into second-generation INSTIs led to the discovery of a tricyclic hydroxypyrrole, MK-2048, which retains the metal binding pharmacophore and the halogenated benzyl moiety found in most INSTIs, but possesses second generation resistance profile (Bar-Magen et al., 2010; Serrao et al., 2009). We used MK-2048 and compound G (Cmpd G; Wai et al., 2007) as benchmark second generation INSTIs, to study the engagement of the catalytic metals in the active site in the context of mutations conferring resistance to first generation inhibitors and to enhance our understanding on the mechanistic basis of resistance to INSTIs.

In vitro resistance selection (IVRS) can be used to identify resistance pathways that may be selected in patients receiving the drug. In most cases, IVRS experiments are initiated with wild-type HIV-1 virus, often laboratory-adapted reference strains such as HXB2-D, IIIB and NL4.3. However, viruses harboring baseline IN sequences from clinical isolates may offer a more representative approach for studying resistance pathways for INSTIs compared with viruses harboring the wild-type IN sequence from a reference strain, and this approach may result in identification of the resistance pathways selected in patients. In this work, we sought to establish whether IVRS initiated with viruses with identical IN sequences would lead to selection of consistent mutations in IN during IVRS and during patient treatment. Therefore, recombinant viruses were produced containing IN sequences of viruses isolated from patients at baseline (initiation) of their RAL-treatment, in a wild-type HIV-1 HXB2 backbone. IVRS experiments with RAL and MK-2048 were initiated with viruses containing known baseline IN sequences from the clinical isolates, and resistant viruses were genotyped, phenotyped and compared with the viruses harboring the IN sequences isolated at virological failure. The cross-resistance to MK-2048 conferred by resistance mutations observed during IVRS, and an extensive analysis of resistance to RAL and MK-2048 of 766 clonal viruses containing IN sequences isolated at virological failure from 106 RAL-treated patients was also performed. To provide insight into the mechanisms of resistance conferred by known mutations we generated HIV-1 homology models incorporating RAL, MK-2048 and key active site features, revealed in recent PFV integrase crystal structures (Hare et al., 2010a,b) and assessed the likely effects on inhibitor binding.

2. Materials and methods

2.1. Anti-viral compounds

Elvitegravir (EVG, GS-9137 (Sato et al., 2006)); Raltegravir (RAL, MK-0518 (Anker and Corales, 2008)); L-870,810 (Hazuda et al., 2004); PACA (a 3-Hydroxy-4-oxo-4,6,7,8,9,10-hexahydro-pyrimido[1,2-a]azepine-2-carboxylamide (Belyk et al., 2006)); PICA (a 9H-Pyrido[3,4-b]indole-3-carboxamide (Kuki et al., 2005)); Compound G (6R)-2-[(3-chloro-4-fluorophenyl)methyl]-8-ethyl-1,2,6,7,8,9-hexahydro-10-hydroxy-N,6-dimethyl-1,9-dioxo-yrazino[1′,2′:1,5]pyrrolo[2,3-d]pyridazine-4-carboxamide (Cmpd G (Wai et al., 2007)) and MK-2048 (Vacca et al., 2007); and the nucleoside reverse transcriptase inhibitor Zidovudine (AZT (Horwitz et al., 1964)). All INSTIs and AZT were chemically synthesized in-house. Chemical structures are shown in Fig. 1.

2.2. Cells and viruses

The human T-lymphoblastoid cell line MT4 was kindly provided by Dr. Naoki Yamamoto (National Institute of Infectious Diseases, AIDS Research Center, Tokyo, Japan). The cell line was maintained in RPMI 1640 medium supplemented with 10% heat-inactivated fetal calf serum, 2 mM L-glutamine, 0.1% $NaHCO_3$, antibiotics (0.02% gentamycin), and stored in a humidified incubator with a 5% CO_2 atmosphere at 37 °C.

MT4–LTR–EGFP cells were obtained by transfecting MT4 cells with a selectable construct encompassing the coding sequences for the HIV-long terminal repeat (LTR) as a promoter for the expression of enhanced green fluorescent protein (EGFP) and subsequent selection of permanently transfected cells.

HIV-1 (IIIB) was provided by Dr. Guido Van der Groen (Institute of Tropical Medicine, Antwerp, Belgium).

2.3. Production of replication-competent recombinant viruses from plasma samples

Plasma samples from four RAL-treated HIV-1 infected patients were selected from the Virco BVBA repository immediately prior to the initiation (baseline) of their RAL-treatment and at the time of treatment failure (where RAL remained in the regimen at the time of sampling, Table 1). All samples were obtained with Informed Consent Form and all links between data and patients are disconnected. Replication-competent recombinant viruses were produced containing the IN sequences of viruses isolated from four patients at baseline (baseline viruses: 1/B, 2/B, 3/B and 4/B, at commencement of RAL-treatment) and at virological failure (failure viruses: 1/F, 2/F, 3/F, 4a/F and 4b/F) in a wildtype HIV-1 HXB2 backbone (Table 1) as described previously (Van Baelen et al., in press). Furthermore, 129 plasma aliquots obtained with Informed Consent Form from 106 RAL-treated patients at virological failure were selected from the Virco BVBA repository and yielded 766 clonal viruses.

For the production of the viruses, viral RNA was extracted either from 256 μl plasma using an automated QIAamp virus BioRobot MDx extraction platform (Qiagen) or from 600 μl plasma using the EasyMag procedure (bio-Mérieux), according to the manufacturers' instructions. cDNA was generated using Accuscript high-fidelity reverse transcriptase (Stratagene) with random hexamers (Invitrogen). Subsequently, the IN gene was amplified by nested PCR using forward primers 5'INoutR1 (positions 4059 to 4081 in HXB2; GenBank accession number K03455) and 5'ININF1 (positions 4143 to 4164 in HXB2) and reverse primers 3'INoutR2 (positions 5241 to 5262 in HXB2) and 3'ININR1 (positions 5195 to 5217 in HXB2). Both the outer and inner PCRs were performed

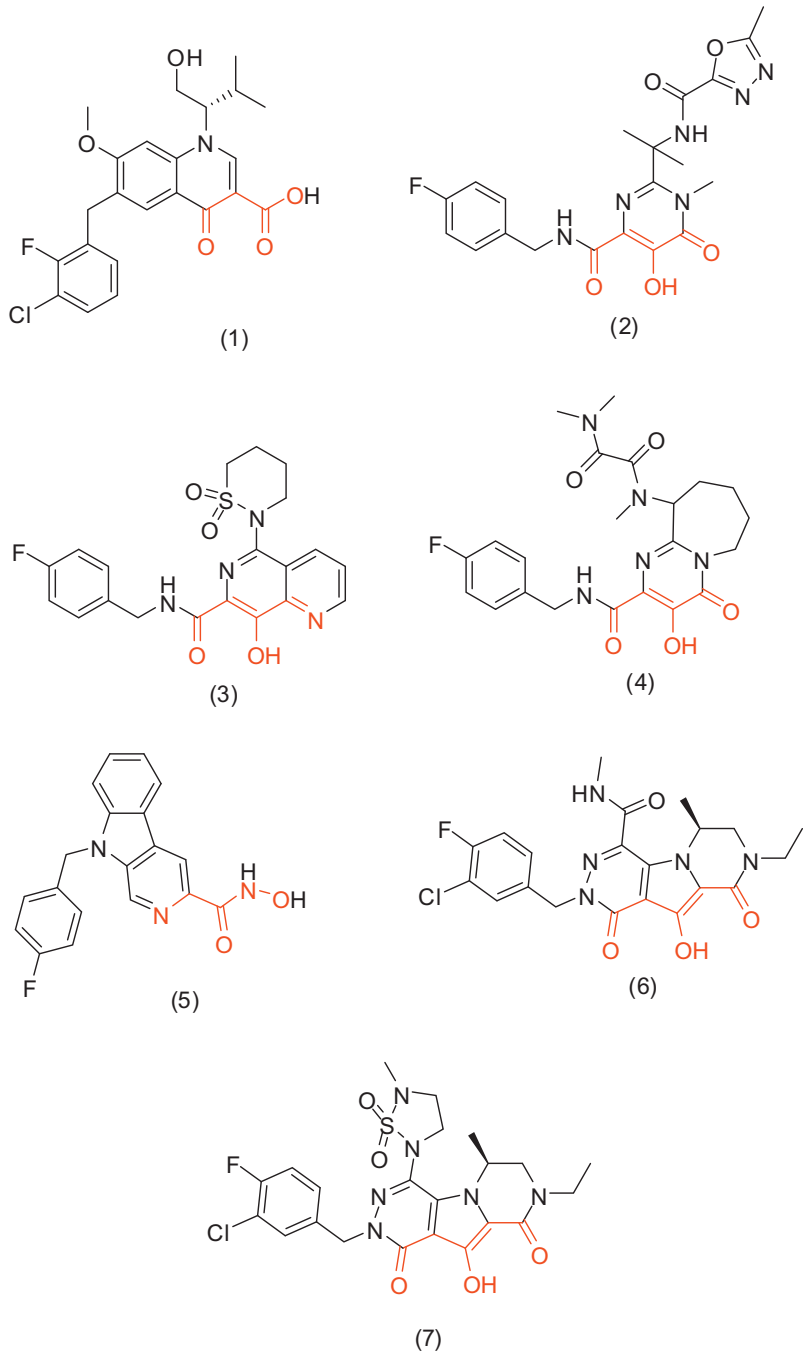

Fig. 1. Structure of seven distinct INSTIs used in this study: EVG (1), RAL (2), L-870,810 (3), PACA (4), PICA (5), MK-2048 (6) and Cmpd G (7). The essential pharmacophore of these compounds is highlighted in red.

using the Phusion high-fidelity PCR master mix (Finnzymes). Thermal cycling of both PCRs consisted of a denaturation step at 98 °C for 30 s; 30 cycles of 10 s at 98 °C, 30 s at 58 °C, and 30 s at 72 °C; and a final elongation for 10 min at 72 °C. Amplicons were purified using the QIAquick PCR purification kit (Qiagen). The purified IN amplicons were cloned into an HXB2-based HIV-1 backbone in which the IN region was deleted (i.e. pHXB2-ΔIN) using In-Fusion Dry-Down PCR cloning technology. Cloning mixes were transformed into MAX Efficiency Stbl2 cells (Invitrogen) using the manufacturer's procedure. Either all colonies were washed off the LB agar transformation plate (population phenotyping; samples at baseline or at RAL-treatment failure from the four patients), or single colonies were picked (clonal phenotyping; 766 clonal viruses) for DNA preparation. Full length recombinant HIV-genome plasmids were prepared using the QiaPrep Spin Miniprep system (Qiagen). Replication-competent recombinant viruses then were generated by Amaxa nucleofection (Amaxa Biosystems, Cologne, Germany) of full-length HIV-genome plasmids into MT4 cells following the manufacturer's recommendations. The cytopathic effect was monitored during the course of infection. When full cytopathic effect was reached, recombinant viruses were harvested by centrifugation.

2.4. Antiviral assays

The antiviral activity of inhibitors was determined in a cell-based HIV-1 replication assay. Briefly, MT4–LTR–EGFP cells were infected with HIV-1 (IIIB, baseline, failure, clonal and selected

Table 1
IN sequences from viruses obtained from plasma samples at baseline (B) or at virological failure (F) or from IVRS with RAL or MK-2048. Primary resistance mutations of RAL or EVG are bold and underlined; secondary resistance mutations of RAL are underlined but not bold.

Clinical sample	Virus name	Virus history	Month	D003	K007	D010	E011	S017	R020	M022	D025	V031	S039	D041	**T66**	V072	L074	T097	L101	K111	T112	I113	S119	T122	G123	A124	T125	V126	R127
1	Virus 1/B	Baseline	M0			E			K							I			I						S	T			K
	Virus 1/F	Failure	M12			E			K							I									S	T			K
	Virus 1/ RAL	RAL selection	M6			E			K						**K**	I	M		I		I/T				S	T			K
	Virus 1/ MK-2048	M K-2048 selection	M8			E			K							I			I		I/T				S	T			K
2	Virus 2/B	Baseline	M0			E		N								I				T			P		S	N	A	L	K
	Virus 2/F	Failure	M12			E		N					R			I	L/M	A/T		T			P		S	N	A	L	K
	Virus 2/ RAL	RAL selection	M6			E		N								I		A		T			P		S	N	A	L	K
	Virus 2/ MK-2048	MK-2048 selection	M8			E		N						D/N		I				T			P		S	N	A	L	K
3	Virus 3/B	Baseline	M0		Q	G	D			L	E	I				I							P	I	S	T	A		K
	Virus 3/F	Failure	M15		Q	G	D			L	E	I				I		A	I				P	I	S	T	A		K
	Virus 3/ MK-2048	MK-2048 selection	M8		Q	G	D			L	E	I				I							P	I	S	T	A		K
4	Virus 4/B	Baseline	M0		R	E		N								I			I			V	P	I/T	S	N	A		K
	Virus 4a/ F	Failure	M3	D/E	K/R	E		N						D/N		I			I			V	P	I/T	S	N	A		K
	Virus 4b/ F	Failure	M10		R	E		N								I			I			V	P		S	N	A		K
	Virus 4/ RAL	RAL selection	M6		R	E		N								I	M		I			V	P	I	S	N	A		K
	Virus 4/ MK-2048	MK-2048 selection	M8		R	E		N								I			I			V	P		S	N	A		K

Clinical sample	Virus name	Virus history	Month	I135	E138	F139	G140	**Y143**	**Q148**	V151	S153Y	M154	**N155**	L158	K160	G163	D167	V201	I203	T206	K219	I220	N222	S230	N232	D253	D256	S283
1	Virus 1/B	Baseline	M0															I				I/L			D			
	Virus 1/F	Failure	M12			F/Y	S		**H**						R			I							D			
	Virus 1/ RAL	RAL selection	M6															I						R/S	D/N			
	Virus 1/ MK-2048	M K-2048 selection	M8								Y					G/R		I							D			
2	Virus 2/B	Baseline	M0																I/M						D		E	
	Virus 2/F	Failure	M12	V						I			**H**						M						D	D/N	E	
	Virus 2/ RAL	RAL selection	M6					**C**		I			**H**											R	D		E	
	Virus 2/ MK-2048	MK-2048 selection	M8																					R	D		E	
3	Virus 3/B	Baseline	M0																						D			G/S
	Virus 3/F	Failure	M15					**R**																	D			G/S
	Virus 3/ M K-2048	MK-2048 selection	M8																						D			
4	Virus 4/B	Baseline	M0									I					E	I			N		K		D			
	Virus 4a/F	Failure	M3		D/E							I	**H**				E	I/V		S/T	N		K		D			
	Virus 4b/F	Failure	M10				S		**H**			I					E	I			N		K		D			
	Virus 4/ RAL	RAL selection	M6					**R**		I		I	**H**	V			E	I			N		K		D/N			
	Virus 4/ MK-2048	MK-2048 selection	M8									I	**H**			R	E	I			N		K		D			

viruses, multiplicity of infection of 0.0025) in the presence or absence of inhibitor. After 4 days of incubation, the inhibition of HIV replication was quantified by a cell viability assay. A resazurin solution (0.1 mg of resazurin/ml, 1 mM $K_4Fe(CN)_6$, and 1 mM $K_3Fe(CN)_6$ in 0.1 mM potassium phosphate buffer; pH 7.4) was added to the cells. Bioreduction of the resazurin dye by viable, metabolically active cells reduces the amount of its oxidized form (blue) and concomitantly increases the amount of its fluorescent intermediate resofurin (red), indicating the degree of inhibition. The amount of dye conversion in solution was measured fluorometrically and the EC_{50} (inhibitor concentration required for 50% inhibition of HIV-1 replication in cell culture) values for each condition was calculated. The cytotoxicity of inhibitors was determined in parallel on mock-infected MT4–LTR–EGFP cells (200,000 cells/ml) cultured in the presence or absence of test compound concentrations. After 4 days of incubation, inhibition of cell proliferation was quantified by the same cell viability assay using resazurin. The rate of dye reduction is directly proportional to the number of viable cells present and is expressed as the CC_{50} (compound concentration that inhibits cell growth by 50%).

2.5. Genotyping

Genotyping was performed by automated population-based full-sequence analysis as described previously (Goethals et al., 2008). Sequencing results were reported as amino acid changes compared with the HIV-1 (HXB2D) wild-type reference sequence. Mutations present in more than 25% of the total virus population were detected as a mixture with the wild type virus.

2.6. Automated IVRS experiments in 96-well plates

In vitro resistance selection was performed in 96-well plates as described previously (Goethals et al., 2008), where each row represented a separate IVRS experiment. In contrast with the classical IVRS experiment, where the compound concentration is only increased at viral breakthrough, this method uses a protocol where the virus is challenged with an increased compound concentration at each passage.

2.7. Molecular modeling

Homology models of HIV IN complexed with DNA and various inhibitors were constructed. The foundation of our models was the structure of the catalytic core domain of HIV IN (PDB ID 1BL3 (Maignan et al., 1998)). This template was modified by incorporation of key elements of the IN active site (flexible loop residues 140–149, α-helix residues 139–158 including active site residue E152, catalytic magnesium ions and coordinated water molecules and 3'-processed DNA and bound inhibitor) as described recently for various PFV IN–DNA–INSTI complex structures (Hare et al., 2010a,b). For our models we used the S217Q PFV IN–DNA–MK-2048 structure (PDB ID 3OYJ; (Hare et al., 2010b)), since this mutant is a better match for wild-type HIV IN (PFV S217Q corresponds to HIV Q148). For RAL complexes, the bound inhibitor was taken from the related PFV IN complex structure, and the side chain conformation of Y143 was manually adjusted to allow π-stacking between the phenol ring of Y143 and the methyl-oxadiazole substituent of RAL, as observed in the PFV IN complex (PDB ID 3OYA; (Hare et al., 2010b)). Side-chains were manually altered to build similar models for the T066I, Y143C, Q148R, S153Y and N155H mutants. All modeled HIV IN complexes were optimized with the protein preparation tool in Maestro (v 9.0; Schrodinger) (Schrödinger, 2009).

3. Results

3.1. Selection and genotype of HIV-1 strains resistant to RAL or MK-2048

An automated parallel IVRS approach in 96-well plates (Goethals et al., 2008) was used to select drug-resistant strains with RAL or MK-2048 initiated with the four baseline viruses. In parallel, HXB2 wild-type virus was used as a control to initiate IVRS with MK-2048 (data not shown). IVRS with drugs was performed during 26 weeks to a final concentration of 5 μM RAL (500-fold EC_{50}(RAL)) and during 34 weeks to a final concentration of 1.6 μM MK-2048 (500-fold EC_{50}(MK-2048)), where viruses were genotyped to identify mutations in their IN sequence (Table 1). During IVRS with MK-2048 and wild-type HXB2D virus, no primary mutations were selected during 8 months of incubation with drug (data not shown), consistent with the previously reported results after 5 months of selection with MK-2048 (Goethals et al., 2010). No primary resistance mutations of RAL were detected in the four baseline viruses used in our study, but several known IN polymorphisms were observed, including V072I and A124T (Table 1). Polymorphisms where present in the baseline samples, remained constant throughout treatment and also in the *in vitro* studies.

Mutations Q148H and G140S, together with additional mutations K160R and F139F/Y, were observed in virus 1/F, while IVRS with RAL and virus 1/B, selected T066K, L074M and T112T/I (virus 1/RAL). IVRS with MK-2048 and virus 1/B, selected S153Y, with two mixtures T112T/I and G163G/R (virus1/MK-2048) (Table 1).

From virus 2/B, primary mutation N155H and additional mutations T097A and V151I were detected after virological failure (virus 2/F) and IVRS with RAL (virus 2/RAL). In addition, virus 2/RAL harbored Y143C, and S230R, where in virus2/F the additional mutations S039R, L074L/M and I203M were also observed. After IVRS with MK-2048 and virus2/B, D041D/N and S230R were present (virus 2/MK-2048) (Table 1).

During IVRS with RAL and virus 3/B, the virus was unable to establish replication (Table 1), therefore no results were obtained. Mutations T097A, L101I and Y143R were observed in virus 3/F, where after IVRS with MK-2048 and virus 3/B, no further mutations were observed (virus 3/MK-2048).

Two plasma samples were obtained from patient 4, one at 12 weeks (virus 4a/F) and one at 40 weeks (virus 4b/F) of RAL-treatment. The primary mutation N155H was observed in virus 4a/F, where Q148H was observed with G140S in virus 4b/F. During 24 weeks of IVRS with RAL and virus 4/B, N155H was selected with L074M, Y143R, V151I and L158V (virus 4/RAL), correlating with the emergence of the N155H mutation after 12 weeks of RAL-treatment (virus 4a/F). Furthermore, IVRS with MK-2048, (virus 4/MK-2048) elicited N155H and G163R (Table 1).

Interestingly, where the N155H mutation arose *in vivo*, IVRS also selected for N155H (samples 2 and 4), yet there are also inconsistencies with resistance mutations at 148 arising *in vivo* in the case of sample 1.

3.2. Phenotypic (cross)-resistance of the RAL- or MK-2048-selected HIV-1 strains to a panel of INSTIs

The viruses isolated at failure of RAL-treatment and the RAL- or MK-2048-selected viruses were phenotyped to determine their susceptibility to RAL, MK-2048 and a panel of INSTIs (EVG, PACA, L-870,810, PICA and Cmpd G) (Fig. 2A–C).

Viruses 1/F and 4b/F, both harboring Q148H, were greatly reduced in susceptibility to all INSTIs, except to Cmpd G. Viruses 2/F and 4a/F (both containing the N155H mutation) showed large reductions in susceptibility to most INSTIs, but not to PICA,

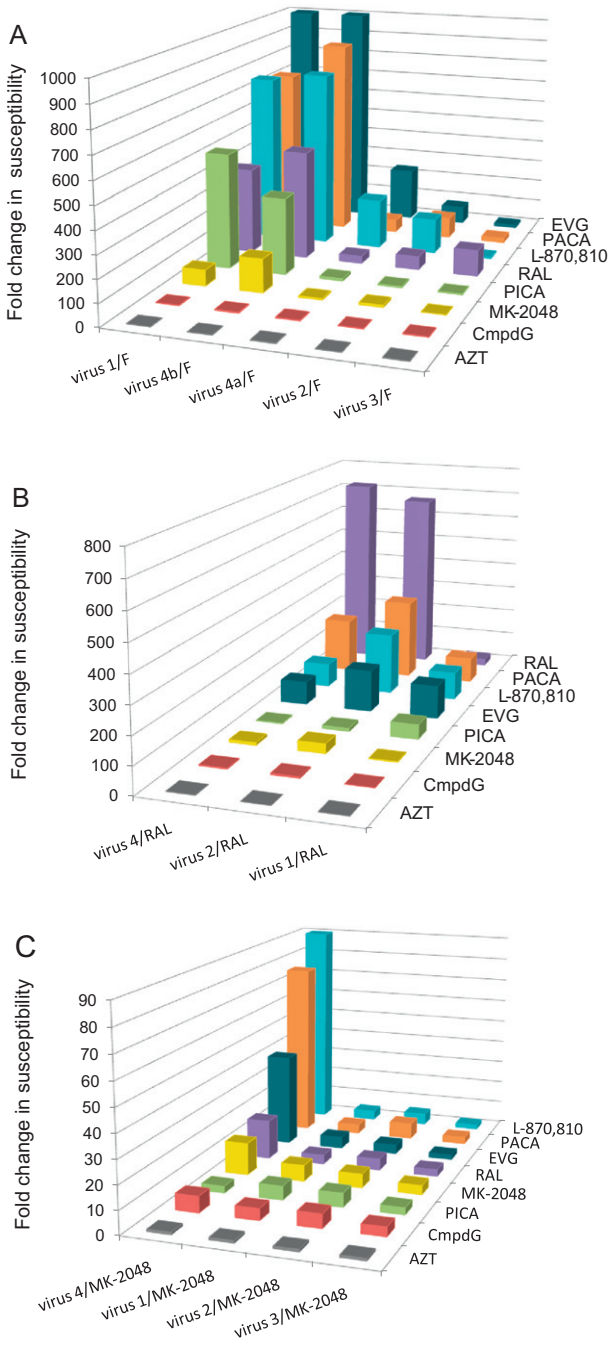

Fig. 2. Phenotyping of resistant mutants and relative changes in susceptibility of all viruses shown as compared with their respective baseline viruses. (A) Cross-resistance of five recombinant HIV-1 viruses with the IN-sequence of four viruses isolated from four patients on a RAL regimen at the time of virological failure, (Table 1) tested for susceptibility to RAL, MK-2048 and other INSTIs and the NRTI AZT; (B) cross-resistance of three RAL-selected HIV-1 strains from three baseline viruses, tested for susceptibility to RAL, MK-2048 and other INSTIs and the NRTI AZT; (C) cross-resistance of four MK-2048-selected HIV-1 strains from baseline viruses tested for susceptibility to RAL, MK-2048 and other INSTIs and the NRTI AZT.

MK-2048 and Cmpd G. Virus 3/F (with mutation Y143R) was reduced in susceptibility to RAL and PACA, but less to the other INSTIs (Fig. 2A).

Compared with their corresponding baseline virus, all three RAL-selected viruses (virus 1/RAL, virus 2/RAL and virus 4/RAL) showed significant resistance to PACA, L-870,810 and EVG (>80-fold). In addition, virus 2/RAL and virus 4/RAL (both harboring N155H) showed large reductions in susceptibility to RAL, while virus 1/RAL (harboring T066K) conferred only a small reduction in susceptibility to RAL.

IVRS with MK-2048 elicited fewer mutations than IVRS with RAL, even though IVRS with MK-2048 was more protracted than with RAL (34 versus 26 weeks, respectively) (Table 1). In virus 1/MK-2048 mutations S153Y and G163G/R were observed, while in virus 2/MK-2048 mutations D041D/N, T112T/I and S230R were elicited. The mutation T112I was previously selected *in vitro* with MK-2048 (Wai et al., 2007), where G118R and E138K have also been reported previously to confer resistance to MK-2048 (Bar-Magen et al., 2010). In addition, previous studies have demonstrated that D041N, T112I, S153Y, G163R and S230R occur as natural polymorphisms of IN (Ceccherini-Silberstein et al., 2009; Lataillade et al., 2007) and confer low resistance to INSTIs. Therefore it is not surprising that virus 1/MK-2048 and virus 2/MK-2048, which harbored in their sequence combinations of these polymorphisms, showed only small reductions in susceptibility to all INSTIs (Fig. 2C). Virus 3/MK-2048 retained the baseline sequence and consequently wild-type susceptibility to all INSTIs. However, virus 4/MK-2048 contained mutations N155H and G163R, and showed large reductions in susceptibility to PACA, L-870,810 and EVG, with more moderate reductions in susceptibility to RAL and MK-2048 (17- and 14-fold, respectively, Fig. 2C).

Small or no reductions (<7-fold) in susceptibility to Cmpd G were observed for the viruses selected during IVRS with RAL or MK-2048, or viruses isolated at virological failure (Fig. 2A–C), similar to previous observations (Goethals et al., 2010; Vacca et al., 2007; Wai et al., 2007).

3.3. Ex vivo genotypic and phenotypic resistance of RAL and (cross)-resistance to MK-2048

To assess cross-resistance to MK-2048 conferred by mutations arising at virological failure with RAL, 766 replication-competent recombinant clonal viruses were produced in an HIV-1 HXB2-backbone, harboring complete IN sequences (positions 4143 to 5217 in HXB2) isolated from 106 RAL-treated patients at virological failure. As these viruses were derived from single colonies (as described in the section 2), several viruses were produced starting from each plasma sample. This could result in viruses with identical IN sequences.

The three main pathways Y143C/R, Q148H/K/R and N155H associated with *in vivo* resistance to RAL were present in our panel of clinical samples. All viruses were phenotyped for susceptibility to RAL and MK-2048 (Fig. 3). Most viruses with genotype N155H (yellow cluster) showed a small to moderate reduction in susceptibility to RAL (FC between 4 and 10) and almost wild-type susceptibility to MK-2048 (FC < 4). Nevertheless, some viruses with N155H showed increased resistance to RAL (10 < FC < 130) and MK-2048 (4 < FC < 30) and also harbored T097A and I203M. As T097A and I203M are considered polymorphisms (Ceccherini-Silberstein et al., 2009), they were omitted from the graph. Viruses with mutation N155H with additional mutations (L074M or E092Q), showed reduced susceptibility to RAL, but almost no change in susceptibility to MK-2048. Viruses harboring Y143C/R (Fig. 3, blue cluster) showed reductions in susceptibility to RAL (FC between 7 and 100), but remained susceptible to MK-2048 (FC < 4). Viruses with Q148H/K/R (Fig. 3, pink cluster) were reduced in susceptibility to RAL (FC ~100) and MK-2048 (FC between 4 and 250). The combination of mutations Q148R, L074M and G140A in one virus conferred a large reduction in susceptibility to MK-2048 (FC ~250). The presence of both L074M and E092Q conferred a large reduction in susceptibility to RAL (FC > 40), with wild-type susceptibility to MK-2048, where the single E092Q mutation reduced the susceptibility to RAL by less than 20-fold.

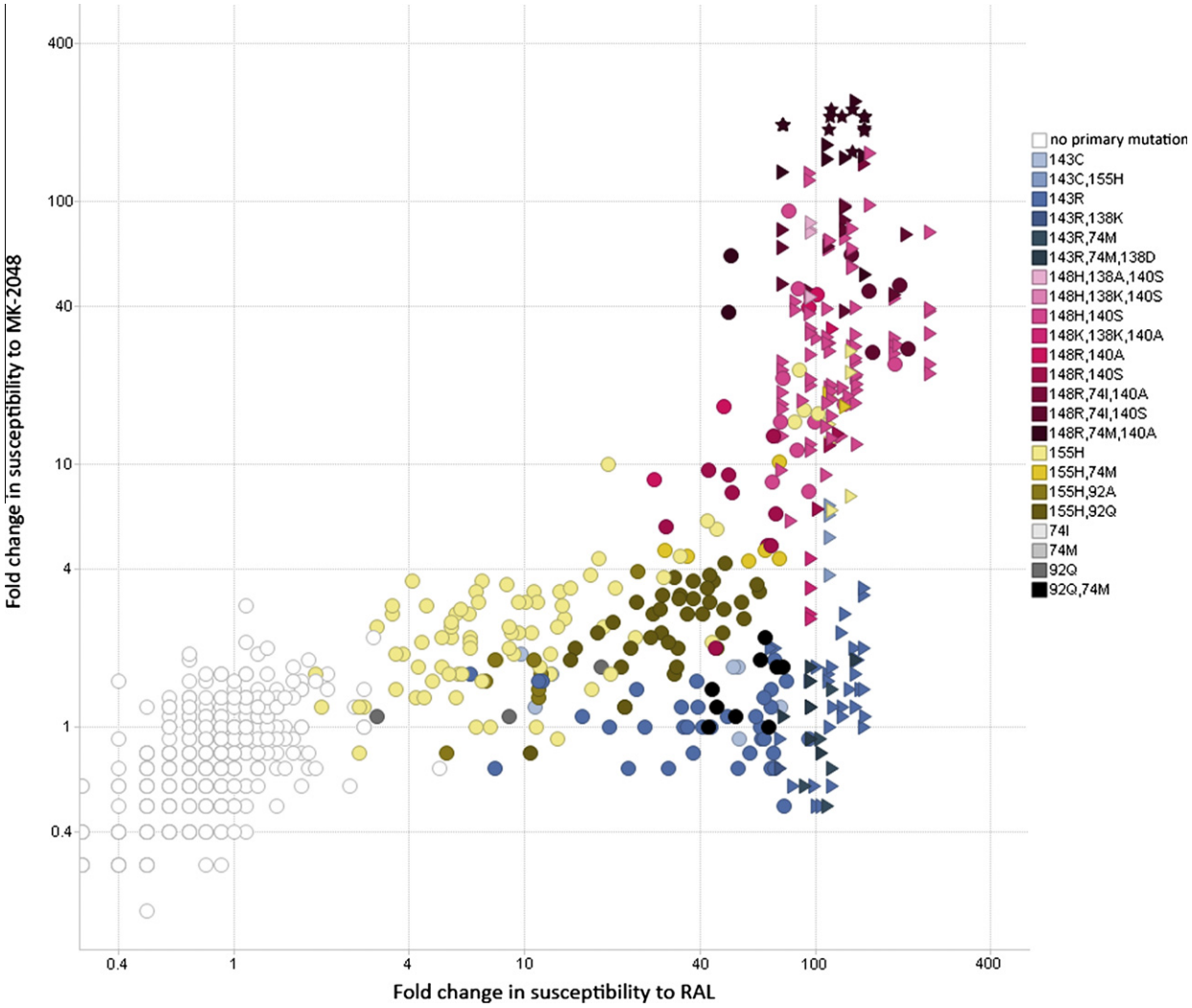

Fig. 3. Scatter plot of fold changes in susceptibility of 766 clonal HIV-1 viruses to RAL and MK-2048. 766 recombinant clonal viruses, with the IN sequence of HIV viruses isolated from 106 RAL-experienced patients were analyzed for their susceptibility to RAL and MK-2048. The genotype of the different viruses is displayed by color codes presented at the right of the graph. Relative changes in susceptibility of the viruses compared with wild-type HIV-1 (HXB2) virus, expressed as fold changes in susceptibility (FC), are displayed on the graph. Symbols: colored circle (O), denotes phenotype where FC to RAL and MK-2048 are equal (=) to the number displayed on the graph; horizontal triangle (▷) denotes phenotype where FC to RAL is greater than (>) the number displayed on the graph, but FC to MK-2048 is equal (=) to the number displayed on the graph; Star (☆) denotes phenotype where FC to both RAL and MK-2048 is greater than (>) the number displayed on the graph.

In summary, our results highlight the three pathways of evolution of resistance to RAL that results from mutations at amino acids 143, 148 and 155, and secondary mutations associated with the Q148 pathway that confer cross-resistance to MK-2048.

3.4. Three-dimensional homology model of full length HIV-1 IN with RAL

Cherepanov and colleagues recently reported an extensive set of PFV IN–DNA and PFV IN–DNA–INSTI crystal structures (Hare et al., 2010a,b; Maertens et al., 2010). These structures have revealed what is believed to be the biologically relevant INSTI binding mode, in which the bound inhibitor displaces the reactive 3' end of the bound viral DNA from the IN active site. The high level of structural and sequence conservation between PFV and HIV INs, most notably in the active site region (Engelman and Craigie, 1992; Kulkosky et al., 1992; Valkov et al., 2009), facilitates relatively straightforward modeling of the analogous HIV-1 IN–DNA and HIV-1 IN–DNA–INSTI complexes (Krishnan et al., 2010; Tang et al., 2010). In the present study we built models based on an earlier HIV-1 IN structure (PDB ID 1BL3 (Maignan et al., 1998)), incorporating key active site elements from the recently disclosed PFV IN structures to yield what appear to be plausible models of the biologically relevant HIV-1 IN–DNA and IN–DNA–INSTI complexes (Fig. 4). Importantly, we extracted PFV IN active site elements from the PFV IN S217Q mutant structure, since this mutant is equivalent to HIV-1 wild type (Q148) at this position. Our models maintain the key active site structural features of the PFV templates, with the metal-coordinating oxygen atoms of the bound INSTIs contacting the active site Mg^{2+} ions and the halobenzyl group occupying a tight pocket created by the displacement of the 3' terminal adenosine of the viral DNA. In addition to models of the wild-type HIV-1 IN complexes, we also built models of several mutant forms (T066I, Y143C, Q148H, S153Y and N155H) of the HIV-1 IN–DNA–RAL and IN–DNA–MK-2048 complexes (the IN–DNA–MK-2048 complex is only shown for Y143 and C143).

With the exception of S153, the residues of interest are clustered around the catalytic DDE-motif of IN. In our HIV-1 IN models (but not in the PFV IN structures, where this residue is I130) the side chain of T066 forms a hydrogen bond with the phosphate of the terminal residue of the 3' processed DNA. This phosphate makes an indirect contact with the Mg^{2+} coordinated by E152

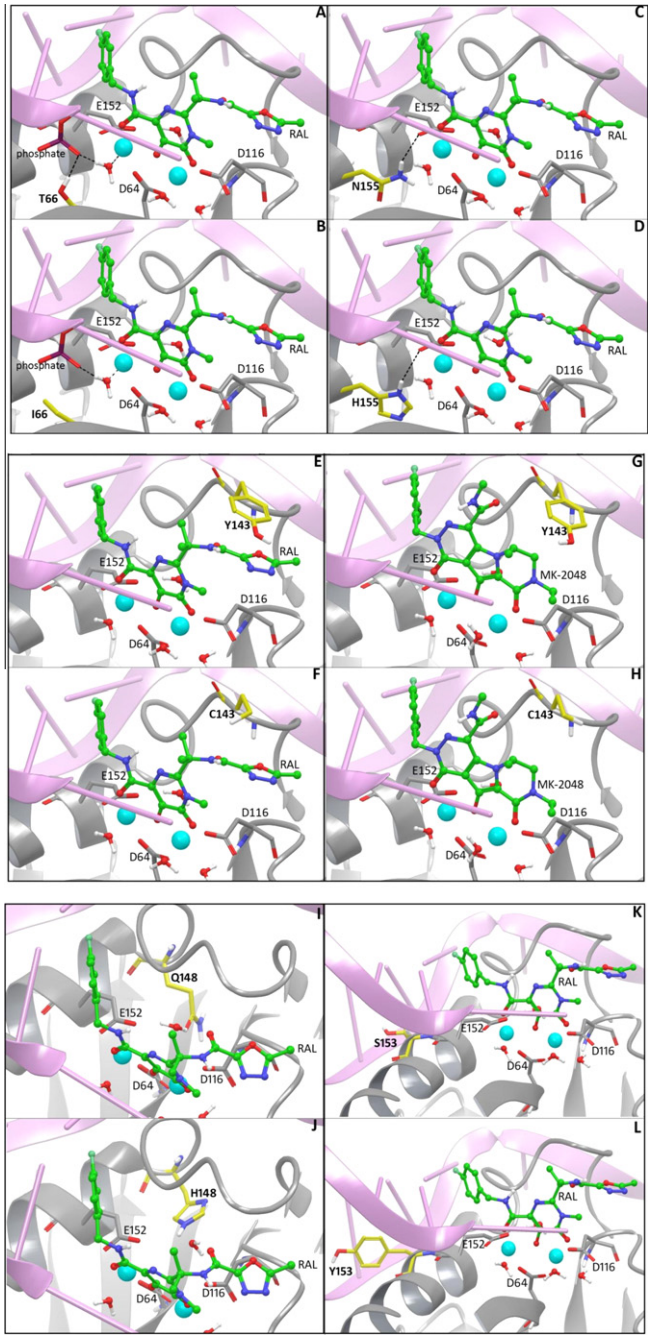

Fig. 4. Three-dimensional homology models of full-length HIV-1 IN in complex with viral DNA and RAL or MK-2048. These models were based on the crystal structure of full length IN from the prototype foamy virus in complex with its cognate DNA and MK-2048 solved by Hare et al. (2010b). The wild-type residues (T066, Y143, Q148, S153 and N155) were visualized and their corresponding mutations (T066I, Y143C, Q148R, S153Y and N155H) were modeled, and their respective interactions with the DNA, enzyme or drug (RAL or MK-2048) were shown; wild-type residue T066 (A), mutation T066I (B), wild-type residue N155 (C), mutation N155H (D), wild-type residue Y143 (E and G), mutation Y143C (F and H), wild-type residue Q148 (I), mutation Q148H (J), wild-type residue S153 (K) and mutation Y153 (L). The Mg^{2+} ions are presented in cyan and the terminal 3'-processed DNA end is shown in pink, with the adenine the last base of the 3'-processed end.

and D064, through a water-mediated hydrogen bonding network (Fig. 4A). T066I is unable to form the hydrogen bond observed for T066, affecting the coordination of the catalytic Mg^{2+} ions through loss of this hydrogen bond and/or steric clash (Fig. 4B).

Y143 and Q148 are both located in the flexible loop, where Y143 interacts directly with RAL through π-stacking of the aromatic phenol sidechain of Y143 with the methyl-oxadiazole ring of RAL (Fig. 4E). Mutation Y143C prevented this interaction, leaving the methyl-oxadiazole moiety of RAL exposed to the solvent (Fig. 4F). However, MK-2048 does not contain an aromatic group comparable with the oxadiazole group of RAL and consequently, MK-2048 does not engage in π-stacking with Y143 for binding to the target complex (Fig. 4G/H), which may explain the wild-type susceptibility of the virus with the Y143C/R mutation to MK-2048 (Goethals et al., 2010).

Analysis of the full set of PFV IN complexes led to the conclusion that mutations at the PFV positions equivalent to HIV-1 IN Q148 and N155, (S217 and N224 in PFV, respectively), achieved their impact through a combination of effects, many of which are relatively subtle (Hare et al., 2010b). Since the present models are based on the PFV IN S217Q mutant, they already have effectively accounted for some of the movement required for INSTI binding by the PFV IN S217H mutant (Hare et al., 2010b). Accommodation of the bulkier and electrostatically distinct Q148H mutant requires multiple minor conformational adjustments in the metal-binding region of the active site, consistent with an altered electronic environment in the region of INSTI coordination to the catalytic Mg^{2+} ions as well as with differential effects on distinct INSTI chemotypes (Fig. 4I/J). In our HIV-1 IN-DNA-INSTI models we observed the formation of a hydrogen bond between N155 and E152 (Fig. 4C). While N155H can maintain this contact (Fig. 4D), this change likely alters the electronic character of the catalytic region, thus impacting the key binding interaction involving INSTI coordination to the active site Mg^{2+} ions.

S153 is positioned near the invariant viral DNA bases that interact with the halobenzyl group of the bound INSTIs (Fig. 4K). Mutation S153Y will likely interfere with the π-stacking interaction observed between the viral DNA base and the halobenzyl group (Fig. 4L).

4. Discussion

RAL is the first HIV-1 INSTI approved by the FDA for use in naïve and treatment-experienced patients. However, the discovery of next-generation antiretrovirals with improved potencies, higher genetic barriers and superior resistance profiles represents an important challenge for drug discovery. In the first part of our study we test whether resistance selection with viruses with known baseline IN sequences would lead to selection of mutations in IN during IVRS that were consistent with those arising during treatment.

At virological failure, each of the four patients harbored one of the canonical RAL resistance mutations; patient 1 harbored mutations Q148H and G140S; patients 2 and 3 had viruses with N155H and Y143R mutations, respectively; the virus from patient 4 switched over time from the N155H to Q148H + G140S, similar to a report from Malet et al. (2009). Clonal genotyping of the isolated viruses from 4a/F and 4b/F showed that Q148H and N155H mutations were present largely on different HIV-1 strains, suggesting that these two pathways are exclusive, consistent with previous data (Malet et al., 2009).

The Y143C/H/R resistance pathway of RAL was observed in a minority of resistant strains in the BENCHMRK studies (Cooper et al., 2008). We selected Y143C/R with RAL in two of four viruses (2/RAL and 4/RAL), in addition to the primary N155H mutation (Table 1). A minority of strains first developed Y143C/H/R IN mutations and then switched to Q148H/K/R, or developed the N155H IN mutation and switched to Y143C/H/R (Da Silva et al., 2008; McColl and Chen, 2010). Viruses 2/RAL and 4/RAL harbored the two

primary mutations (N155H + Y143C or Y143R, respectively). Possibly during protracted IVRS with RAL, N155H could disappear and Y143R/C/H could remain as observed in the clinical studies. We have previously shown that N155H conferred a greater reduction in susceptibility to RAL and other INSTIs than Y143C (Goethals et al., 2010). A switch from N155H to Y143C is therefore not explained by an increased resistance of Y143C compared with N155H; it is possible, however, that viral evolution was influenced by diminished replicative capacity conferred by the N155H mutation (Goethals et al., 2008). We report the selection of N155H after IVRS with MK-2048, suggesting a similar mechanism of resistance to RAL and MK-2048. Furthermore, mutation S153Y was observed in virus 1/MK-2048. Interestingly, S153F/Y changes were reported during IVRS with the second generation INSTI GSK-1349572 (Sato et al., 2009).

IVRS experiments initiated with baseline viruses 2/B and 4/B with RAL led to the consistent selection of N155H, *in vivo* and *in vitro*, indicating the value of IVRS in profiling the resistance pathways of INSTIs. During IVRS with virus 4/B and MK-2048, the N155H mutation was also selected (Table 1), suggesting some correlation between the selection of resistance mutations in IN during therapy and IVRS, when initiated with viruses with identical IN sequences. For example, naturally occurring polymorphisms or the prevalence of minority variants could lead to more rapid selection of a particular mutation during drug-pressure. Charpentier et al. (2010) showed that Q148R variants were frequently detected in INSTI-naïve patients where it is reasonable to speculate that the Q148R mutation would emerge more rapidly under RAL pressure than in a patient lacking the Q148R quasispecies.

In the second part of this study, 766 recombinant viruses were produced harboring the IN sequence isolated from 106 RAL-experienced patients and were phenotyped for susceptibility to RAL and cross-resistance to MK-2048 (Fig. 3). These viruses were made based on single colonies. Therefore, viruses with identical IN sequences could be produced. The phenotypes of these identical viruses were similar and served as a good control of the reproducibility of our phenotype assay. Nevertheless, we observed that all major RAL-associated mutations (Q148K/H/R, N155H and Y143R/C) were present in our database of recombinant viruses. Most viruses with the Q148H/K/R mutation (pink cluster) showed a large reduction in susceptibility to RAL and generally a larger than tenfold reduction in susceptibility to MK-2048, consistent with the phenotypes of virus 1/F and virus 4/F, both harboring Q148H and G140S, and highlighting the clinical relevance of this pathway.

Cherepanov and colleagues recently reported X-ray structures of full-length PFV IN bound to viral DNA ends and INSTIs (Hare et al., 2010a,b), enabling the construction of realistic models for the active and drug-inhibited forms of the HIV-1 intasome. Homology models of several HIV-1 IN–DNA–INSTI complexes, including those of the mutant INs and the corresponding wild-type INs were built and offer relatively straightforward explanations for the effects of some resistance mutations (Fig. 4), while the mechanisms of others remain somewhat speculative.

Y143 interacts directly with RAL by π-stacking of the aromatic group from the tyrosine at 143 and the methyl-oxadiazole moiety of RAL. Disruption of this specific π–π contact in Y143C/R is fully consistent with both the reduced RAL susceptibility observed for these mutants as well as the lack of impact observed for MK-2048 (Goethals et al., 2010), which lacks an equivalent π-stacking group.

Significant conformational adjustment was observed for the set of S217Q/H PFV IN complexes, especially so for the MK-2048 complexes, where certain resistance effects were ascribed to the protein conformational adjustment required for inhibitor binding (Hare et al., 2010b). By using the S217Q PFV IN structure as the basis of our HIV-1 IN models, we accounted for most of this motion in our "parent" HIV-1 IN model. While less pronounced, we nonetheless observed similar adjustment in the backbone conformation of our HIV-1 IN models in the region of residues 148 and 155 upon inhibitor binding. PFV mutation N224H, corresponding to N155H of HIV-1 IN, interacted with the phosphate of the terminal adenine of bound viral DNA, resulting in the absence of one of the bound metal cofactors in the absence of a bound INSTI (Hare et al., 2010b). This change is consistent with both the reduced replicative capacity observed for the N155H mutant and the reduced susceptibility to INSTIs (Goethals et al., 2008, 2010).

Since IN binding of all known INSTIs likely relies on coordination to both catalytic Mg^{2+} cations, it may be that mutation of T066, N155 or Q148 will cause a reduction in susceptibility to many INSTIs, further underlining the need for more resistance data and the extrapolation of the genotype to phenotype, and thus the correlation with the chemical scaffold and resistance is clearly a priority in the discovery of INSTIs with exemplary resistance profiles. Indeed, it is probable that the susceptibility of mutants to a specific INSTI depends on the Mg^{2+} coordinating capacity of the INSTI in the "mutated" electric field around the catalytic Mg^{2+} cations. The Mg^{2+}-coordinating pharmacophore of second-generation INSTIs, e.g. MK-2048 and GSK-1349572 (Vandeckerckhove, 2010), is part of a larger polarizable group consisting of a semi conjugated tricyclic ring system. An electronically and/or geometrically adaptable metal binding functionality may be a prerequisite for a second-generation INSTI resistance profile.

In summary, we highlight the consistency between the *in vivo* and *in vitro* resistance profiles for INSTIs and underline the value of IVRS as a tool for predicting resistance profiles of antiretrovirals during discovery and development, and enhance our understanding of the mechanism of resistance of RAL associated mutations.

Acknowledgements

The authors gratefully acknowledge Dr. Peter Cherepanov and Dr. Steven Hare for providing the coordinates of the PFV intasome structure and for many helpful discussions during the preparation of the manuscript.

References

(No authors listed), 2008. Phase III trial begins for elvitegravir. AIDS Patient Care STDS 22, 762–763.
(No authors listed), 2009. FDA notifications. FDA approves raltegravir for HIV-1 treatment-naive patients. AIDS Alert 24, 106–107.
Anker, M., Corales, R.B., 2008. Raltegravir (MK-0518): a novel integrase inhibitor for the treatment of HIV infection. Expert. Opin. Investig. Drugs 17, 97–103.
Bar-Magen, T., Sloan, R.D., Donahue, D.A., Kuhl, B.D., Zabeida, A., Xu, H., Oliveira, M., Hazuda, D.J., Wainberg, M.A., 2010. Identification of novel mutations responsible for resistance to MK-2048, a second-generation HIV-1 integrase inhibitor. J. Virol. 84, 9210–9216.
Belyk, K.M., Morisson, H.G., Jones, P., Summa, V., 2006. Potassium salt of an HIV integrase inhibitor. Merck, Patent WO2006060712.
Ceccherini-Silberstein, F., Malet, I., D'Arrigo, R., Antinori, A., Marcelin, A.G., Perno, C.F., 2009. Characterization and structural analysis of HIV-1 integrase conservation. AIDS Rev. 11, 17–29.
Charpentier, C., Laureillard, D., Piketty, C., Tisserand, P., Batisse, D., Karmochkine, M., Si-Mohamed, A., Weiss, L., 2010. High frequency of integrase Q148R minority variants in HIV-infected patients naive of integrase inhibitors. AIDS 24, 867–873.
Chen, I.J., Neamati, N., MacKerell Jr., A.D., 2002. Structure-based inhibitor design targeting HIV-1 integrase. Curr. Drug Targets Infect. Disord. 2, 217–234.
Clavel, F., Hance, A.J., 2004. HIV drug resistance. N. Engl. J. Med. 350, 1023–1035.
Cocohoba, J., 2009. The SWITCHMRK studies: substitution of lopinavir/ritonavir with raltegravir in HIV-positive individuals. Expert Rev. Anti. Infect. Ther. 7, 1159–1163.
Cooper, D.A., Steigbigel, R.T., Gatell, J.M., Rockstroh, J.K., Katlama, C., Yeni, P., Lazzarin, A., Clotet, B., Kumar, P.N., Eron, J.E., Schechter, M., Markowitz, M., Loutfy, M.R., Lennox, J.L., Zhao, J., Chen, J., Ryan, D.M., Rhodes, R.R., Killar, J.A., Gilde, L.R., Strohmaier, K.M., Meibohm, A.R., Miller, M.D., Hazuda, D.J., Nessly, M.L., DiNubile, M.J., Isaacs, R.D., Teppler, H., Nguyen, B.Y., 2008. Subgroup and resistance analyses of raltegravir for resistant HIV-1 infection. N. Engl. J. Med. 359, 355–365.

Da Silva, D., Pellegrin, I., Anies, G., Breilh, D., Wittkop, L., Morlat, P., Dupon, M., Neau, D., Pellegrin, J.L., Fleury, H., Masquelier, B., 2008. Mutations patterns in the HIV-1 integrase related to virological failure on raltegravir-containing regimens, XVII International HIV Drug Resistance Workshop, Sitges, Spain.

DeGruttola, V., Dix, L., D'Aquila, R., Holder, D., Phillips, A., Ait-Khaled, M., Baxter, J., Clevenbergh, P., Hammer, S., Harrigan, R., Katzenstein, D., Lanier, R., Miller, M., Para, M., Yerly, S., Zolopa, A., Murray, J., Patick, A., Miller, V., Castillo, S., Pedneault, L., Mellors, J., 2000. The relation between baseline HIV drug resistance and response to antiretroviral therapy: re-analysis of retrospective and prospective studies using a standardized data analysis plan. Antivir. Ther. 5, 41–48.

Engelman, A., Craigie, R., 1992. Identification of conserved amino acid residues critical for human immunodeficiency virus type 1 integrase function in vitro. J. Virol. 66, 6361–6369.

Eron, J.J., Young, B., Cooper, D.A., Youle, M., Dejesus, E., Andrade-Villanueva, J., Workman, C., Zajdenverg, R., Fatkenheuer, G., Berger, D.S., Kumar, P.N., Rodgers, A.J., Shaughnessy, M.A., Walker, M.L., Barnard, R.J., Miller, M.D., Dinubile, M.J., Nguyen, B.Y., Leavitt, R., Xu, X., Sklar, P., 2010. Switch to a raltegravir-based regimen versus continuation of a lopinavir–ritonavir-based regimen in stable HIV-infected patients with suppressed viraemia (SWITCHMRK 1 and 2): two multicentre, double-blind, randomised controlled trials. Lancet 375, 396–407.

Esposito, D., Craigie, R., 1999. HIV integrase structure and function. Adv. Virus Res. 52, 319–333.

Goethals, O., Clayton, R., Van Ginderen, M., Vereycken, I., Wagemans, E., Geluykens, P., Dockx, K., Strijbos, R., Smits, V., Vos, A., Meersseman, G., Jochmans, D., Vermeire, K., Schols, D., Hallenberger, S., Hertogs, K., 2008. Resistance mutations in human immunodeficiency virus type 1 integrase selected with elvitegravir confer reduced susceptibility to a wide range of integrase inhibitors. J. Virol. 82, 10366–10374.

Goethals, O., Vos, A., Van Ginderen, M., Geluykens, P., Smits, V., Schols, D., Hertogs, K., Clayton, R., 2010. Primary mutations selected in vitro with raltegravir confer large fold changes in susceptibility to first-generation integrase inhibitors, but minor fold changes to inhibitors with second-generation resistance profiles. Virology 402, 338–346.

Hare, S., Gupta, S.S., Valkov, E., Engelman, A., Cherepanov, P., 2010a. Retroviral intasome assembly and inhibition of DNA strand transfer. Nature 464, 232–236.

Hare, S., Vos, A.M., Clayton, R.F., Thuring, J.W., Cummings, M.D., Cherepanov, P., 2010b. Molecular mechanisms of retroviral integrase inhibition and the evolution of viral resistance. Proc. Natl. Acad. Sci. USA. 107, 20057–20062.

Hazuda, D.J., Anthony, N.J., Gomez, R.P., Jolly, S.M., Wai, J.S., Zhuang, L., Fisher, T.E., Embrey, M., Guare Jr., J.P., Egbertson, M.S., Vacca, J.P., Huff, J.R., Felock, P.J., Witmer, M.V., Stillmock, K.A., Danovich, R., Grobler, J., Miller, M.D., Espeseth, A.S., Jin, L., Chen, I.W., Lin, J.H., Kassahun, K., Ellis, J.D., Wong, B.K., Xu, W., Pearson, P.G., Schleif, W.A., Cortese, R., Emini, E., Summa, V., Holloway, M.K., Young, S.D., 2004. A naphthyridine carboxamide provides evidence for discordant resistance between mechanistically identical inhibitors of HIV-1 integrase. Proc. Natl. Acad. Sci. USA 101, 11233–11238.

Hazuda, D.J., Felock, P., Witmer, M., Wolfe, A., Stillmock, K., Grobler, J.A., Espeseth, A., Gabryelski, L., Schleif, W., Blau, C., Miller, M.D., 2000. Inhibitors of strand transfer that prevent integration and inhibit HIV-1 replication in cells. Science 287, 646–650.

Horwitz, J., Chua, J., Noel, M., 1964. Nucleosides V. The monomesylates of 1-(2'-deoxy-bèta-D-lyxofuranosyl)thymidine. J. Org. Chem. 29, 2076–2078.

Johnson, V.A., Brun-Vezinet, F., Clotet, B., Gunthard, H.F., Kuritzkes, D.R., Pillay, D., Schapiro, J.M., Richman, D.D., 2009. Update of the drug resistance mutations in HIV-1: December 2009. Top HIV Med. 17, 138–145.

Krishnan, L., Li, X., Naraharisetty, H.L., Hare, S., Cherepanov, P., Engelman, A., 2010. Structure-based modeling of the functional HIV-1 intasome and its inhibition. Proc. Natl. Acad. Sci. USA. 107, 15910–15915.

Kuki, A., Li, X., Plewe, M.B., Wang, H., Zhang, J., 2005. HIV-integrase inhibitors, pharmaceutical compositions, and methods for their use. In: Agouron Pharmaceuticals, I., Patent US2005165040.

Kulkosky, J., Jones, K.S., Katz, R.A., Mack, J.P., Skalka, A.M., 1992. Residues critical for retroviral integrative recombination in a region that is highly conserved among retroviral/retrotransposon integrases and bacterial insertion sequence transposases. Mol. Cell Biol. 12, 2331–2338.

LaFemina, R.L., Schneider, C.L., Robbins, H.L., Callahan, P.L., LeGrow, K., Roth, E., Schleif, W.A., Emini, E.A., 1992. Requirement of active human immunodeficiency virus type 1 integrase enzyme for productive infection of human T-lymphoid cells. J. Virol. 66, 7414–7419.

Lataillade, M., Chiarella, J., Kozal, M.J., 2007. Natural polymorphism of the HIV-1 integrase gene and mutations associated with integrase inhibitor resistance. Antivir. Ther. 12, 563–570.

Lennox, J.L., Dejesus, E., Berger, D.S., Lazzarin, A., Pollard, R.B., Ramalho Madruga, J.V., Zhao, J., Wan, H., Gilbert, C.L., Teppler, H., Rodgers, A.J., Barnard, R.J., Miller, M.D., Dinubile, M.J., Nguyen, B.Y., Leavitt, R., Sklar, P., 2010. Raltegravir versus efavirenz regimens in treatment-naive HIV-1-infected patients: 96-week efficacy, durability, subgroup, safety, and metabolic analyses. J. Acquir. Immune Defic. Syndr. 55, 39–48.

Lennox, J.L., DeJesus, E., Lazzarin, A., Pollard, R.B., Madruga, J.V., Berger, D.S., Zhao, J., Xu, X., Williams-Diaz, A., Rodgers, A.J., Barnard, R.J., Miller, M.D., DiNubile, M.J., Nguyen, B.Y., Leavitt, R., Sklar, P., 2009. Safety and efficacy of raltegravir-based versus efavirenz-based combination therapy in treatment-naive patients with HIV-1 infection: a multicentre, double-blind randomised controlled trial. Lancet 374, 796–806.

Maertens, G.N., Hare, S., Cherepanov, P., 2010. The mechanism of retroviral integration from X-ray structures of its key intermediates. Nature 468, 326–329.

Maignan, S., Guilloteau, J.P., Zhou-Liu, Q., Clement-Mella, C., Mikol, V., 1998. Crystal structures of the catalytic domain of HIV-1 integrase free and complexed with its metal cofactor: high level of similarity of the active site with other viral integrases. J. Mol. Biol. 282, 359–368.

Malet, I., Delelis, O., Soulie, C., Wirden, M., Tchertanov, L., Mottaz, P., Peytavin, G., Katlama, C., Mouscadet, J.F., Calvez, V., Marcelin, A.G., 2009. Quasispecies variant dynamics during emergence of resistance to raltegravir in HIV-1-infected patients. J. Antimicrob. Chemother. 63, 795–804.

McColl, D., Fransen, S., Gupta, S., Parkin, N., Margot, N., Chuck, S., Cheng, A., Miller, M., 2007. Resistance analysis of a Phase 2 study of the integrase inhibitor elvitegravir (GS-9137), 11th European Aids Conference, Madrid, Spain.

McColl, D.J., Chen, X., 2010. Strand transfer inhibitors of HIV-1 integrase: bringing IN a new era of antiretroviral therapy. Antiviral Res. 85, 101–118.

Neamati, N., Lin, Z., Karki, R.G., Orr, A., Cowansage, K., Strumberg, D., Pais, G.C., Voigt, J.H., Nicklaus, M.C., Winslow, H.E., Zhao, H., Turpin, J.A., Yi, J., Skalka, A.M., Burke Jr., T.R., Pommier, Y., 2002. Metal-dependent inhibition of HIV-1 integrase. J. Med. Chem. 45, 5661–5670.

Palella Jr., F.J., Delaney, K.M., Moorman, A.C., Loveless, M.O., Fuhrer, J., Satten, G.A., Aschman, D.J., Holmberg, S.D., 1998. Declining morbidity and mortality among patients with advanced human immunodeficiency virus infection. HIV outpatient study investigators. N. Engl. J. Med. 338, 853–860.

Paredes, R., Clotet, B., 2010. Clinical management of HIV-1 resistance. Antiviral Res. 85, 245–265.

Pommier, Y., Johnson, A.A., Marchand, C., 2005. Integrase inhibitors to treat HIV/AIDS. Nat. Rev. Drug Discov. 4, 236–248.

Richman, D.D., 2001. HIV chemotherapy. Nature 410, 995–1001.

Richman, D.D., 2006. Antiviral drug resistance. Antiviral Res. 71, 117–121.

Sakai, H., Kawamura, M., Sakuragi, J., Sakuragi, S., Shibata, R., Ishimoto, A., Ono, N., Ueda, S., Adachi, A., 1993. Integration is essential for efficient gene expression of human immunodeficiency virus type 1. J. Virol. 67, 1169–1174.

Sato, A., Kobayashi, M., Yoshinaga, T., Fujiwara, T., Underwood, M., Johns, B., Foster, S., Hazen, R., Ferris, R., Brown, K., 2009. S/GSK1349572 integrase inhibitor resistance profile, 12th European AIDS conference, Cologne, Germany.

Sato, M., Motomura, T., Aramaki, H., Matsuda, T., Yamashita, M., Ito, Y., Kawakami, H., Matsuzaki, Y., Watanabe, W., Yamataka, K., Ikeda, S., Kodama, E., Matsuoka, M., Shinkai, H., 2006. Novel HIV-1 integrase inhibitors derived from quinolone antibiotics. J. Med. Chem. 49, 1506–1508.

Schrödinger, 2009. Suite Protein Preparation Wizard; Epik version 2.0, Schrödinger, LLC, New York, NY, 2009; Impact version 5.5, Schrödinger, LLC, New York, NY, 2009; Prime version 2.1, Schrödinger, LLC, New York, NY, 2009.

Serrao, E., Odde, S., Ramkumar, K., Neamati, N., 2009. Raltegravir, elvitegravir, and metoogravir: the birth of "me-too" HIV-1 integrase inhibitors. Retrovirology 6, 25.

Tang, J., Maddali, K., Pommier, Y., Sham, Y.Y., Wang, Z., 2010. Scaffold rearrangement of dihydroxypyrimidine inhibitors of HIV integrase: docking model revisited. Bioorg. Med. Chem. Lett. 20, 3275–3279.

Vacca, J.P., Wai, J.S., Fisher, T.E., Embrey, M., Hazuda, D.J., Miller, M.D., Felock, P.J., Witmer, M.V., Gabryelski, L., Lyle, T., 2007. Discovery of MK-2048: subtle changes confer unique resistance properties to a series of tricyclic hydroxypyrrole integrase strand transfer inhibitors, 4th International AIDS Society (IAS) Conference, Sydney, Australia.

Valkov, E., Gupta, S.S., Hare, S., Helander, A., Roversi, P., McClure, M., Cherepanov, P., 2009. Functional and structural characterization of the integrase from the prototype foamy virus. Nucleic Acids Res. 37, 243–255.

Van Baelen, K., Rondelez, E., Van Eygen, V., Ariën, K., Clynhens, M., Van den Zegel, P., Winters, B., Stuyver, L.J., 2009. A combined genotypic and phenotypic human immunodeficiency virus type1 recombinant virus assay for the reverse transcriptase and integrase genes. J. Virol. Methods 161, 231–239.

van Gent, D.C., Mizuuchi, K., Gellert, M., 1996. Similarities between initiation of V(D)J recombination and retroviral integration. Science 271, 1592–1594.

Vandeckerckhove, L., 2010. GSK-1349572, a novel integrase inhibitor for the treatment of HIV infection. Curr. Opin. Investig. Drugs 11, 203–212.

Wai, J.S., Fisher, T.E., Embrey, M., Egbertson, M.S., Vacca, J.P., Hazuda, D.J., Miller, M.D., Witmer, M.V., Gabryelski, L., Lyle, T., 2007. Next Generation of Inhibitors of HIV-1 Integrase Strand Transfer Inhibitor: Structural Diversity and Resistance Profiles. CROI, Los Angeles, California.